PERGAMON Mechanics and Physics of Solids 47 (1999) 141–172

JOURNAL OF THE MECHANICS AND PHYSICS OF SOLIDS

Thermal trapping and kinetics of martensitic phase boundaries

Shing-Chung Ngan, Lev Truskinovsky*

Department of Aerospace Engineering and Mechanics, University of Minnesota, Minneapolis, MN 55455, U.S.A.

Received 13 November 1997; revised 28 May 1998

Abstract

In this paper we study the influence of latent heat on kinetics of martensitic phase transitions and derive a relation between the velocity of an adiabatic phase boundary and the corresponding driving force (kinetic relation). Inside the phase transition front we adopt a non-isothermal version of the viscosity-capillarity model. We show that if the latent heat is different from zero, a finite value of the driving force must be reached, before the transition front can move; this effect of thermal trapping may contribute to martensitic hysteresis. In the adiabatic case the kinetic relations are non-monotone and non-single-valued, reproducing some fine features of the kinetic relations obtained previously for purely mechanical discrete models with bi-stable elements. We show that in its gross features, our kinetic model is similar to the conventional model of dry friction.

Keywords: A. Phase transformation; A. Thermomechanical process; A. Dynamic fracture; B. Stress waves; C. Kinetic relations

1. Introduction

The interest in dynamics of phase boundaries in elastic solids is stimulated by the necessity to understand the constitutive rate sensitivity of shape memory alloys. Materials of this type primarily deform through the correlated migration of martensitic phase boundaries and it has become common to model their peculiar behavior in the framework of elasticity theory with non (quasi) convex stored energy. Physically, the non-convexity of elastic energy reflects bi-stability of the constitutive elements.

* Corresponding author.

S0022–5096/98/$ - see front matter
PII: S0022–5096(98)00080–5

Propagation of the phase boundary may then be viewed as an auto-catalytic process of internal buckling or flipping over of these elements; high mobility of the 'switching' waves is a result of the continuity of atomic lattice (no slip) and the associated smallness of the energy barriers.

The objective of the present paper is to study the adiabatic phase boundary propagation in a thermo-elastic bar. The one-dimensional continuum model used for the description of the internal structure of the transitional region includes three coupled partial differential equations, representing the conservation of energy, linear momentum and mass (strain compatibility). The material is considered to be heat conducting, additional dispersive terms are added as in strain gradient elasticity, and non-thermal dissipation is described by Kelvin viscoelasticity (Slemrod, 1983, 1984; Truskinovsky, 1982, 1985). We focus on the traveling wave solutions and obtain an explicit necessary condition of admissibility for subsonic phase boundaries (kinks). This condition, which does not follow from the overall balances on the jump discontinuity, is often referred to as a kinetic relation and has its well known counterpart in dynamic fracture mechanics (Freund, 1990; Truskinovsky, 1993).

There exists a considerable literature on dynamics of martensitic phase boundaries in a purely mechanical setting (e.g. Abeyaratne and Knowles, 1991a,b; Gurtin, 1993; Truskinovsky, 1987, 1997). In this class of models, it is assumed that the removal of heat is instantaneous on the time scale of dynamics and that the motion is controlled by the kinetics of structural transformation. An alternative approach, which dates back to Stefan, assumes that the motion of the phase boundary is governed by the removal or supply of latent heat; in this purely thermal description both structural transformation and stress relaxation are considered instantaneous at the time scale of heat propagation (e.g. Leo et al., 1993; Zhong and Batra, 1996).

Recent experiments with shape memory wires (Shaw and Kiriakides, 1995; Shield et al., 1997) demonstrated unambiguously the influence of thermal effects on the overall rate of phase transformation as well as on the size (and shape) of the hysteresis loop. The theoretical models, based on Stefan's approach, brought some interesting results. Thus, analysis of the traveling waves by Bruno et al. (1995) (see also Malomed and Rumanov, 1985), showed that, in the absence of convective heat exchange with the environment, an isolated interface will be stationary until a certain threshold is reached; then at a critical driving force the interface can move arbitrarily fast. With the convection term included, purely thermal theory successfully reproduces sufficiently slow-rate experiments. At the same time, the infinite speed of transformation at a critical stress is incompatible with the quasistatic approximation which suggests that at least for the simulation of high-strain-rate tests the mechanical description has to be refined.

It is therefore of interest to analyze the dynamics of phase boundaries from the perspective of a more general model of martensitic phase transition which treats simultaneously inertia and heat release. In the realistic case where the thermal boundary layer is much smaller than the size of the body, a phase boundary can be treated as thermally isolated or adiabatic. Although in this approximation heat conductivity is considered only inside the transformation front, the overall kinetics is strongly affected by the rate of redistribution of the latent heat.

Phenomenological kinetic relations for the adiabatic case can be formally considered in a form identical to the case of isothermal phase boundaries (e.g. Abeyaratne and Knowles, 1994b). In an attempt to derive kinetic relations from a micromodel, Slemrod (1984) and Truskinovsky (1985) studied the structure of the adiabatic phase transition waves in the framework of a non-isothermal viscosity–capillarity model under the assumption that the coefficient of heat conductivity is large; Turteltaub (1997) has recently obtained an exact solution in this limiting case for a tri-linear elastic material. Some mathematical results concerning the existence of adiabatic travelling waves outside this asymptotics can be found in the papers by Grinfeld (1989) and Garcke (1995); the topological methods used, however, provided little information about the resulting kinetic relations.

In the present paper we adopt a specific nonlinear stress–strain-temperature model for the two-phase elastic material and study both analytically and numerically the adiabatic kinetic relations in a wide range of nondimensional parameters characterising dissipative and dispersive properties of the material. While we observe a lot of similarities between the isothermal and the adiabatic kinetics, several new important features emerge.

First, in the case of non-zero latent heat, a finite value of the driving force must be reached before the transition front can move (thermal trapping). Second, the relation between the phase boundary velocity and the corresponding driving force turns out to be generically non-monotone. In particular, we observe that, similar to the conventional models of dry friction, the velocity of sufficiently slow phase boundaries may be a decreasing function of the generalized force. This result is interesting in view of a recent paper of Rosakis and Knowles (1997) who showed that the non-monotinicity of the kinetic relation can lead to a stick-slip mode of propagation. For the special case of 'infinite' heat conductivity, similar non-monotonicity of the kinetic relations in the viscosity capillarity model was also observed by Turteltaub (1997). In the closely related non-isothermal Ginzburg–Landau model, the non-monotone character of the relation between the driving force and the interface velocity has been long known (Patashinsky and Chertkov, 1990; Umantzev, 1991).

The most unexpected and previously unnoticed feature of the kinetic relations, originating from the non-isothermal viscosity-capillarity model, is their multi-valuedness at low velocities. Thus, for a given state ahead of the transition front we obtain several travelling wave solutions with internal profiles differing by a number of finite oscillations in the front structure. It is quite remarkable that our adiabatic kinetic relations show close qualitative resemblance to the multi-valued 'force–flux' curves calculated numerically for the 'failure waves' in bi-stable discrete lattices (Slepyan and Troyankina, 1984; Marder and Gross, 1995). Although the latter, purely mechanical models, were developed to simulate radiational aspects of the propagation of cracks, an analogy between fracture and martensitic phase transitions, having its origin in the non-convexity of the elastic energy, makes these discrete calculations extremely relevant for our problem (e.g. Truskinovsky, 1996). The fact that the above multivaluedness in the continuum model disappears when the latent heat of transformation is put equal to zero, suggests an intriguing relation between the discreteness and thermodynamics.

The outline of the paper is as follows. In Section 1 we give the motivation of this work and discuss the necessity of kinetic relations. The equations of the regularized model are derived in Section 2. We then study the traveling wave solutions; the mathematical problem consists of finding a heteroclinic trajectory for the system of ordinary differential equations in 3D phase space. Some interesting special cases that can be studied analytically are considered in Section 3. Numerical results for the general case can be found in Section 4. In Section 5 we reformulate our results in terms of the functional dependence of the rate of dissipation upon the phase boundary velocity. Finally in Section 6 we give conclusions and discuss possible implications for dynamic fracture.

2. Motivation

Consider a simplest longitudinal deformation of a homogeneous bar with unit cross section and let $u(x, t)$ be displacement of a reference point x at time t. Introduce strain $w = u_x$ and particle velocity $v = u_t$, where the subscripts indicate partial derivatives. The standard balance of mass, linear momentum and energy for adiabatic motions take the form

$$w_t = v_x, \quad v_t = \sigma_x, \quad e_t = \sigma v_x, \tag{1.1}$$

where $e(w, s)$ is the specific internal energy (s is the specific entropy) and

$$\sigma = e_w(w,s)$$

is the stress. The referential density is assumed to be equal to unity. When $\sigma_w(w, s) > 0$, the system (1.1) is hyperbolic with three characteristic speeds

$$\lambda = \{0, \pm\sqrt{\sigma_w(w,s)}\}$$

and one cannot expect solutions to stay smooth. On the discontinuities, the system (1.1) must be supplemented by the Rankine–Hugoniot jump conditions

$$D[w]+[v] = 0, \quad D[v]+[\sigma] = 0, \quad D[e+\tfrac{1}{2}v^2]+[\sigma v] = 0, \tag{1.2}$$

where $[\,] = (\,)_+ - (\,)_-$ and D is the Lagrangian speed of propagation of the discontinuity. A convenient form of the jump conditions (1.2) can be obtained if particle velocities are eliminated. Then we get either

$$[\sigma]-D^2[w] = 0, \quad [e]-\{\sigma\}[w] = 0, \tag{1.3}$$

where $\{\,\} = \frac{1}{2}((\,)_+ + (\,)_-)$, or

$$D = 0, \quad [\sigma] = 0, \quad [v] = 0. \tag{1.4}$$

The (degenerate) jumps of the second type, given by eqn (1.4), are called contact discontinuities.

To illustrate relation (1.3), suppose the stress and the strain in front of the discontinuity are prescribed, say (σ_+, w_+). Then eqn (1.3) describes two sets of points on the (σ_+, w_+) plane called the Rayleigh line and the Hugoniot adiabat; the two curves intersect at (σ_+, w_+) and possibly at one or several other points. As it follows from eqn (1.4) the jump transitions described by the contact discontinuities do not have to belong to the same Hugoniot adiabat.

We will characterize material undergoing martensitic phase transformation by the structure of its Hugoniot adiabat and assume that the Rayleigh line and the Hugoniot adiabat may have up to three points of intersection. This configuration is schematically shown in Fig. 1. One can show that when the specific heat at constant strain,

$$c = Ts_T(w, T) \equiv \partial e(w, s(w, T))/\partial T > 0,$$

is sufficiently large, this assumption is a direct consequence of the nonconvexity of the elastic free energy of the material as a function of strain.

For the particular configuration shown in Fig. 1, one can consider two types of jump discontinuities $w_+ \to w^s_-$ and $w_+ \to w^k_-$. Neither of them can be excluded based on the entropy criterion, which reads†

$$-D[s] \geqslant 0.$$

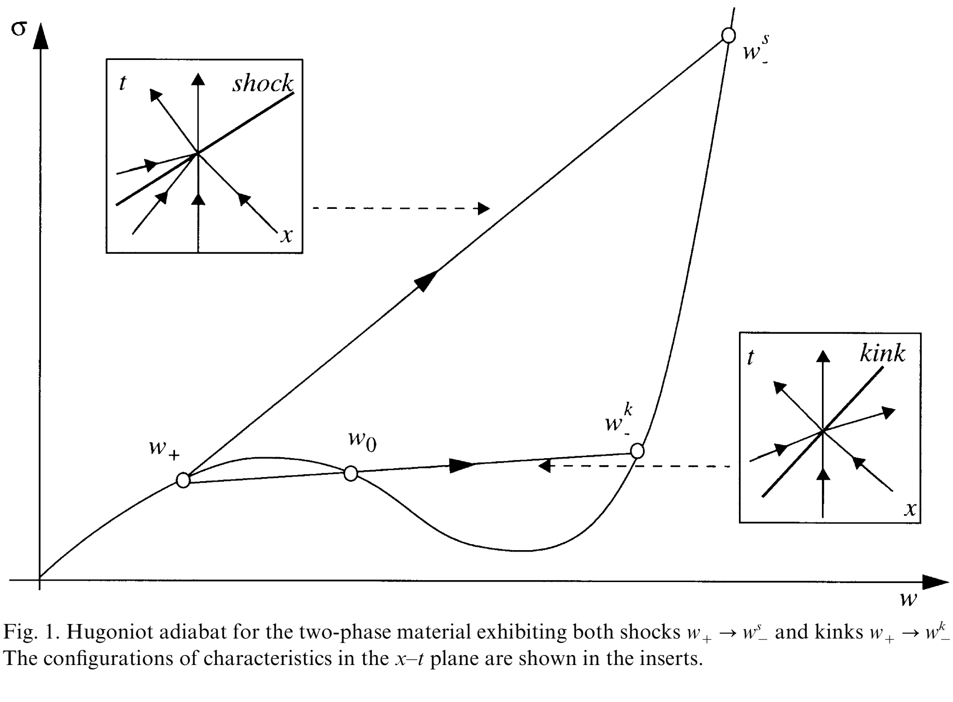

Fig. 1. Hugoniot adiabat for the two-phase material exhibiting both shocks $w_+ \to w^s_-$ and kinks $w_+ \to w^k_-$. The configurations of characteristics in the x–t plane are shown in the inserts.

† Define ΔA as a signed area between the Rayleigh line and the Hugoniot curve; one can show that $\Delta A = \int_{s_+}^{s_-} T\,ds$, where $T = e_s(w, s)$ is the temperature and the integral is taken along the Hugoniot curve. Then, according to the entropy criterion, it is necessary that $\Delta A \geqslant 0$ (for $D \geqslant 0$).

There is, however, an important difference between the two types of jumps. The first discontinuity $w_+ \to w^s_-$, which we call a *shock*, satisfies the Lax criterion (Lax, 1971).

$$a_- \geqslant D \geqslant a_+,$$

where

$$a = \sqrt{\sigma_w(w,s)}$$

is the adiabatic velocity of acoustic waves and

$$D^2 = (\sigma_- - \sigma_+)/(w_- - w_+)$$

is the velocity of the shock. In our case, the Lax condition is equivalent to the statement that four characteristics are entering and two are leaving the shock, which means stable interaction of the discontinuity with acoustic waves (see the insert in Fig. 1). The second transition $w_+ \to w^k_-$, which we call a kink, and which is sometimes referred to as non-evolutionary or under-compressive shock, violates the Lax criterion since

$$a_- \geqslant D \quad \text{and} \quad a_+ \geqslant D.$$

This means that three characteristics are entering and three are leaving which results in an instability unless an additional jump condition is prescribed (see, for instance, Kulikovsky, 1976).

To check the Lax criterion one can use the following relation between the slope of the Hugoniot adiabat and the adiabatic sound speed

$$\left(\frac{d\sigma}{dw}\right)_H - D^2 = (a^2 - D^2)\left(1 + \frac{w - w_+}{2\alpha T}\frac{a^2 - b^2}{b^2}\right)^{-1}.$$

Here the derivative on the left is calculated along the Hugoniot adiabat and we introduced

$$\alpha = w_T(\sigma, T),$$

the coefficient of thermal expansion and

$$b = \sqrt{\sigma_w(w, T)},$$

the isothermal acoustic velocity which is always smaller than the adiabatic acoustic velocity since

$$a^2 = b^2(1 + b^2\alpha^2 T/c).$$

In the most general form, the additional jump relation for kinks can be written as

$$\psi(w_+, w_-, v_+, v_-, T_+, T_-, D) = 0.$$

The Rankine–Hugoniot conditions and Galilean invariance allow one to reduce this formula, at least locally, to a relation among only three variables, say

$$\bar{\psi}(w_+, T_+, D) = 0. \tag{1.5}$$

At the phenomenological level, one can interpret this condition as a postulate about the rate of entropy production at a jump discontinuity.‡ The explicit expression for the dissipation is often formulated in terms of a relation between the thermodynamic 'force'

$$G \equiv -[s]$$

and the conjugate 'flux' D, for example

$$D = H(G); \tag{1.6}$$

moreover, it is sometimes assumed that the function H is linear in D and the dissipative function is quadratic—theory of 'normal growth' (Truskinovsky, 1987, 1994a). Being too special in view of eqn (1.5), a kinetic relation in the form of eqn (1.6) is sometimes modified by the introduction of an explicit dependence on average temperature, say

$$D = H(G\{T\}) \tag{1.7}$$

or more generically

$$D = H(G\{T\},\{T\}),$$

(see, for instance, Abeyaratne and Knowles, 1994a,b). One of the goals of the present paper is to derive a relation in the form of eqn (1.5) from the analysis of the internal structure of the discontinuity and to check the validity of the special phenomenological models leading to eqns (1.6) or (1.7).

3. The model

A purely dissipative regularization is sufficient to describe the structure of shocks. In the case of kinks there exists an additional energetic barrier which material particles have to overcome on their way from one phase to another. In order to describe the process of barrier crossing, one needs a regularization, which contains dispersive terms (Truskinovsky, 1997).

In our model dispersion will be introduced through a strain gradient contribution to the internal energy

$$e = e(w,w_x,s).$$

Then, instead of eqn (1.1) we get

$$w_t = v_x, \quad v_t = (\sigma - m_x)_x, \quad e_t = \sigma v_x + m v_{xx} - q_x.$$

‡The difficulty with the phenomenological approach arises from the fact that the additional jump condition cannot be universally applicable to all jump discontinuities and must differentiate between shocks and kinks. Physically, in the case of shocks, the rate of dissipation is not constrained by the internal process, which only controls the thickness of the interface. Kinks, on the contrary, constitute a class of discontinuities for which the internal structure has less flexibility and the rate of dissipation cannot be prescribed arbitrarily (see Truskinovsky, 1997, for more details).

Here

$$\sigma = e_w(w,w_x,s)$$

is the stress,

$$m = e_{w_x}(w,w_x,s)$$

is the hyperstress (moment) and

$$q = -\kappa T_x$$

is the Fourier heat flux (κ is the coefficient of heat conductivity). The particular strain gradient contribution will be taken in the form

$$e(w,s) = e(w,s)+\varepsilon w_x^2,$$

where ε is a positive parameter which characterizes the degree of nonlocality.

Suppose that in addition to heat conductivity, there exists another dissipative process of kinetic origin inside the transition region, which we will model by a standard (Kelvin) viscosity. This brings an additional contribution to stress in the form

$$\tau = \eta v_x,$$

where η is the viscosity coefficient. With these assumptions, the system (1.1) reads

$$w_t = v_x, \quad v_t = (\sigma(w,s)-2\varepsilon w_{xx}+\eta v_x)_x,$$

$$(e(w,s)+\varepsilon w_x^2+\tfrac{1}{2}v^2)_t = ((\sigma(w,s)-2\varepsilon w_{xx}+\eta v_x)v)_x+2\varepsilon(v_x w_x)_x+\kappa T_{xx}. \quad (2.1)$$

These equations constitute a non-isothermal extension of the viscosity–capillarity model (e.g. Slemrod, 1984).

As a first test of the model, consider stability of a homogenous state. Following the standard procedure, we look for solutions in the form $\exp i(kx-\omega t)$. The dispersion relation reads

$$p^3+p^2\left(1+\frac{\eta}{d}\right)+p\left(\frac{\eta}{d}+\frac{2\varepsilon}{d^2}+\frac{a^2}{k^2d^2}\right)+\left(\frac{2\varepsilon}{d^2}+\frac{b^2}{k^2d^2}\right) = 0,$$

where $d = \kappa/c$ is thermal diffusivity and $p = i\omega/(k^2d)$ is the growth increment. The Hurwitz criterion gives a necessary and sufficient condition of stability. If $\kappa \neq 0$ we get

$$b^2 \geqslant -2\varepsilon k^2,$$

which, in particular, means that for the infinite domain the state is stable if and only if the isothermal acoustic velocity is real, $b^2 \geqslant 0$. A similar result for the case of heat conducting media without viscosity and spatial dispersion was obtained by Abeyaratne and Knowles (1994b). If the coefficient of heat conductivity is identically zero, $\kappa = 0$, it is the adiabatic acoustic speed that has to be real for stability: $a^2 \geqslant 0$. Since always $a^2 \geqslant b^2$, the criterion based on isothermal sound speed is sufficient.

To model the internal structure of the moving interface, consider a special solution of the system (2.1) in the form of a traveling wave

$$w = w(z), \quad v = v(z), \quad T = T(z),$$

where $z = x - Dt$. These three functions must satisfy the following system of ODEs

$$-Dw' = v', \quad -Dv' = (\sigma + \eta v' - 2\varepsilon w'')',$$

$$-D\left(e + \varepsilon w'^2 + \frac{1}{2}v^2\right)' = ((\sigma + \eta v' - 2\varepsilon w'')v)' + 2\varepsilon(v'w')' + \kappa T'', \quad (2.2)$$

where prime denotes differentiation in z. The system (2.2) is considered in the infinite domain with the following boundary conditions:

$$w(\pm\infty) = w_\pm, \quad v(\pm\infty) = v_\pm, \quad T(\pm\infty) = T_\pm.$$

After integrating once, eliminating velocity v and introducing instead a new variable $y = w'$ one can rewrite the system (2.2) in the form

$$w' = y, \quad y' = \frac{1}{2\varepsilon}[\sigma(w, T) - \sigma_+ - \eta Dy - D^2(w - w_+)],$$

$$T' = -\frac{D}{\kappa}\left\{e(w, T) - e_+ - \frac{1}{2}D^2(w - w_+)^2 - \varepsilon y^2 - \sigma_+(w - w_+)\right\}. \quad (2.3)$$

We are interested in heteroclinic trajectories of the system (2.3) and the main problem is to find restrictions on the set of boundary values $w_\pm$, $v_\pm$, $T_\pm$, D, which guarantees the existence of such a solution. After the solution is known, the rate of entropy production can be calculated from

$$-D[s] = \int_{-\infty}^{\infty}\{\kappa(T'/T)^2 + (\eta/T)(v')^2\}\mathrm{d}z.$$

We begin with the characterization of the critical points of the dynamical system (2.3). The coordinates of these points satisfy the Rankine–Hugoniot jump conditions (see eqn (1.2)). The corresponding matrix of the linearized system can be written explicitly

$$A = \begin{bmatrix} 0 & 1 & 0 \\ \{b^2 - D^2\}/2\varepsilon & -\eta D/2\varepsilon & -\alpha b^2/2\varepsilon \\ -\alpha b^2 DT/\kappa & 0 & -Dc/\kappa \end{bmatrix}.$$

The three invariants of A are:

$$S_1(A) = \mathrm{tr}(A) = -D\{\eta/2\varepsilon + c/\kappa\},$$

$$S_2(A) = \tfrac{1}{2}\{(\mathrm{tr}(A))^2 - \mathrm{tr}(A^2)\} = -\{b^2 - D^2(1 + \eta c/\kappa)\}/2\varepsilon,$$

$$S_3(A) = \det(A) = cD\{a^2 - D^2\}/2\varepsilon\kappa.$$

Without the loss of generality assume $D > 0$. By evaluating the three invariants S_1,

S_2 and S_3 at various intersection points of the Rayleigh line and the Hugoniot curve from Fig. 1, we obtain the following characterization:

- Kinks ($w_+ \to w_-^k$): w_+-saddle with 1D unstable manifold ($S_1 < 0$, $S_3 > 0$); w_0-stable node or focus ($S_1 < 0$, $S_2 > 0$, $S_3 < 0$); w_-^k-saddle with 1D unstable manifold ($S_1 < 0$, $S_3 > 0$).
- Shocks ($w_+ \to w_-^s$): w_+-stable node or focus ($S_1 < 0$, $S_2 > 0$, $S_3 < 0$); w_-^s-saddle with 1D unstable manifold ($S_1 < 0$, $S_3 > 0$).

The fact that kinks correspond to saddle–saddle trajectories, while shocks correspond to saddle–node (focus) trajectories is responsible for the difference in the number of admissibility conditions. Suppose that the state in front of the discontinuity $w = w_+$, $T = T_+$ is given. This fixes one of the critical points, and leaves the position of the other one at $w = w_-$, $T = T_-$ unspecified until the speed of the jump D is prescribed. Now, the problem of admissibility can be reformulated as a nonlinear eigenvalue problem with respect to D. Since the saddle to node transition is structurally stable, the spectrum of admissible speeds for the shocks will be continuous. On the other hand, since the saddle to saddle transition is not structurally stable, one obtains at most a discrete set of admissible Ds. The branches of this set constitute what we call a kinetic curve.

In order to be able to do numerical simulations, we have to specify the expression for one of the thermodynamic potentials, for instance the specific free energy $f(w, T)$. We make the simplest assumptions:

(i) Isothermal stress–strain curve is cubic;
(ii) Maxwell stress is a linear function of temperature, $\sigma_M = A + BT$;
(iii) The equilibrium (Maxwell) strains w_1 and w_2 are independent of temperature.

These assumptions lead to the following stress–strain relation

$$\sigma(w, T) = A + BT + K(w - w_1)(w - w_2)(w - \tfrac{1}{2}(w_1 - w_2))$$

where A, B and K are positive constants. If in addition we assume that the specific heat c is constant, we obtain the following explicit expression for the free energy

$$f(w, T) = Aw + BTw + K\left\{\frac{w^4}{4} - \frac{1}{2}(w_1 + w_2)w^3 + \frac{1}{2}w^2\left(\frac{w_1^2}{2} + 2w_1w_2 + \frac{w_2^2}{2}\right) - w_1w_2\left(\frac{w_1 + w_2}{2}\right)w\right\} - cT\ln\frac{T}{T_0}.$$

Here T_0 is some reference temperature. To demonstrate the physical meaning of the parameter B, we calculate expressions for the entropy,

$$s(w, T) = -Bw + c\ln(T/T_0) + c,$$

and for the equilibrium heat effect in the isothermal transformation (latent heat),

$$Q = T(s_2 - s_1) = -B(w_2 - w_1)T.$$

In case $B > 0$, heat is released when material transforms from the low strain phase to the high strain phase; this also means that the equilibrium boundary in stress–temperature space has a positive slope

$$\mathrm{d}\sigma_M/\mathrm{d}T = B \geqslant 0.$$

Now, we can non-dimensionalize the main system of eqn (2.3). Introduce (i) A, the scale of stress; (ii) $\sqrt{\varepsilon}/A$, the scale of length (capillary); (iii) A/c, the scale of temperature. Assume for simplicity that $A = K$ which means that the width of the 'hysteresis' is of the order of Maxwell stress. Then the system of equations will depend on three main non-dimensional parameters:

$$\boldsymbol{W}_1 = \frac{\eta}{\sqrt{\varepsilon}}, \quad \boldsymbol{W}_2 = \frac{c\sqrt{\varepsilon}}{\kappa}, \quad \boldsymbol{W}_3 = \frac{B}{c},$$

where $\boldsymbol{W}_1$ is the ratio of viscosity to capillarity, $\boldsymbol{W}_2$ is the ratio of heat conductivity to capillarity and $\boldsymbol{W}_3$ is a measure of the latent heat. After the velocity field is eliminated, the non-dimensionalized equation (2.2) takes the form

$$\begin{aligned} w'' &= \tfrac{1}{2}\{\sigma(w,T)-\sigma(w_+,T_+)-\boldsymbol{W}_1 D w' - D^2(w-w_+)\},\\ T' &= -D\boldsymbol{W}_2\{e(w,T)-e(w_+,T_+)-\tfrac{1}{2}D^2(w-w_+)^2-w'^2-\sigma(w_+,T_+)(w-w_+)\}. \end{aligned} \tag{2.4}$$

Let us assume for simplicity that

$$w_1 = 0 \quad \text{and } w_2 = 1.$$

Then

$$e(w,T) = w+\tfrac{1}{4}w^4-\tfrac{1}{2}w^3+\tfrac{1}{4}w^2+T-1, \quad \sigma(w,T) = 1+\boldsymbol{W}_3 T+w(w-1)(w-\tfrac{1}{2}). \tag{2.5}$$

Equations (2.4) together with the constitutive relations of eqn (2.5) and the boundary conditions

$$w(\pm\infty) = w_\pm, \quad T(\pm\infty) = T_\pm$$

will be the main focus of our analysis. In the next two sections we present the results of analytical and numerical study of the admissible domains in the (w_+, D) space for the given T_+ and variable $\boldsymbol{W}_1$, $\boldsymbol{W}_2$ and $\boldsymbol{W}_3$.

4. Special cases

In this section we discuss some special cases which give important insights about the generic behavior of the system.

4.1. *Athermal medium* ($\mathbf{W}_3 = 0$)

In this most studied special case the temperature can be eliminated from eqn (2.4) and the problem reduces to a purely mechanical one. Physically the assumption $\boldsymbol{W}_3 = 0$ means either zero latent heat or infinite specific heat; in the latter case the motion is also isothermal. The relative simplicity of this asymptotics is based on the fact that the phase space is two dimensional.

In the isothermal limit, the main system of eqns (2.4) and (2.5) reduces to

$$w' = y, \quad y' = \tfrac{1}{2}[(w-1)(w)(w-\tfrac{1}{2})-(w_+-1)(w_+)(w_+-\tfrac{1}{2})-\boldsymbol{W}_1 D y - D^2(w-w_+)]. \tag{3.1}$$

The boundary conditions are

$$w(-\infty) = w_-, \quad w(\infty) = w_+$$

and the only nondimensional parameter left is $\boldsymbol{W}_1$. There exists a closed form solution describing isothermal kinks (e.g. Truskinovsky, 1987, 1994a)

$$w(z) = \frac{w_+ + w_-}{2} + \frac{w_+ - w_-}{2}\tanh\left\{\frac{w_+ - w_-}{4}(z-z_0)\right\}. \tag{3.2}$$

Parameters w_-, w_+ and the velocity D must satisfy the following relations:

$$(w_- - w_+)^2 + 3(1-12/\boldsymbol{W}_1^2)(w_+ + w_- - 1)^2 = 1, \quad D = 3(w_+ + w_- - 1)/\boldsymbol{W}_1. \tag{3.3}$$

Formulas (3.2) and (3.3) provide the desired kinetic relation in a parametric form (with w_- as a parameter, see eqn (1.5) with T_+ fixed). The generic kinetic curve, shown in Fig. 2, begins at point $A(w_+, T_+)$, which is given implicitly by Maxwell conditions

$$T_+ = T_-, \quad \sigma(w_+, T_+) = \sigma(w_-, T_-),$$
$$e(w_-, T_-) - T_- s_- - e(w_+, T_+) + T_+ s_+ = \sigma(w_+, T_+)(w_- - w_+), \tag{3.4}$$

and ends on a sonic line CE. The sonic line corresponds to (Jouget) shocks that move with a sonic speed with respect to the state ahead and is given explicitly by the equation

$$D = b(w_+) = \sqrt{3w_+^2 - 3w_+ + \tfrac{1}{2}}.$$

The *1D* sub-set of kinks in eqn (3.3) is a part of a bigger admissibility set which includes both kinks and shocks. The generic case is shown in Fig. 2. We notice that only some of the Lax shocks are admissible. In fact, there exists a subset of shocks satisfying the Lax criterion (the domain between the lines OB and OE in Fig. 2) which do not have a viscosity–capillarity structure (see Truskinovsky, 1994b; Shearer and Zang, 1995). The expression for the curve OB, which separates admissible from non-admissible shocks, can be obtained as follows. We have a point on the curve OB if

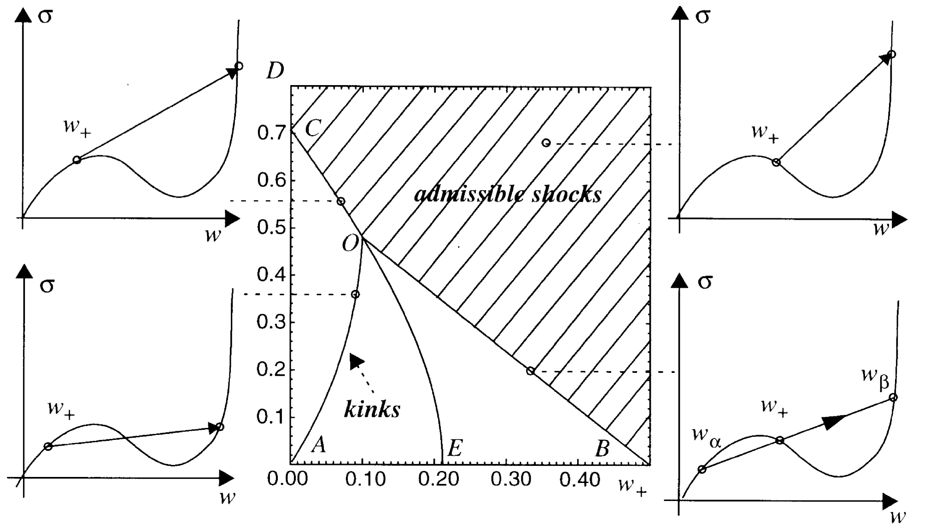

Fig. 2. A generic picture of the domain of admissibility for the isothermal case in $D-w_+$ plane. The $2D$ area bounded by the curve COB corresponds to admissible shocks. The $1D$ segment AO corresponds to kinks. The area EOB corresponds to the domain of non-admissible Lax shocks. The representative discontinuities are shown schematically in the inserts. The state w_+ is in front of the discontinuity. In this figure $\boldsymbol{W}_1 = 2.5$ and $T_+ = 50$.

for the given w_+ there exists a state $w_\beta < w_+$ and another state $w_\alpha > w_+$ such that: (i) the state w_+ is on the Rayleigh line passing through w_β and w_α; (ii) there is a heteroclinic connection from the state w_β to the state w_α which satisfies eqn (3.3). A straightforward calculation gives the following parametric representation for the relation between w_+ and D along the line OB

$$w_\alpha = \frac{1}{-36+4\boldsymbol{W}_1^2}\{-36+3\boldsymbol{W}_1^2+w_\beta(36-2\boldsymbol{W}_1^2) - \boldsymbol{W}_1\sqrt{w_\beta(12\boldsymbol{W}_1^2-144)+w_\beta^2(144-12\boldsymbol{W}_1^2)+\boldsymbol{W}_1^2},$$

$$w_+ = \frac{3}{4}-\frac{w_\beta}{2} + \frac{1}{4\boldsymbol{W}_1}\sqrt{144(1-2w_\alpha+w_\alpha^2-2w_\beta+2w_\alpha w_\beta+w_\beta^2)+\boldsymbol{W}_1^2+12w_\beta\boldsymbol{W}_1^2-12w_\beta^2\boldsymbol{W}_1^2},$$

$$D = 3(w_\alpha+w_\beta-1)/\boldsymbol{W}_1.$$

The behavior of the kinetic curves at various values of $\boldsymbol{W}_1$ is illustrated in Fig. 3. If dissipation dominates dispersion ($\boldsymbol{W}_1 \to \infty$), the kinetic relation reduces to $D = 0$ and all Lax shocks become admissible; this special case was studied by Shearer (1982) and Pego (1987). If dispersion dominates dissipation ($\boldsymbol{W}_1 \to 0$), shocks disappear while the kinetic relation for kinks reduces to the 'equal area' construction (Truskinovsky,

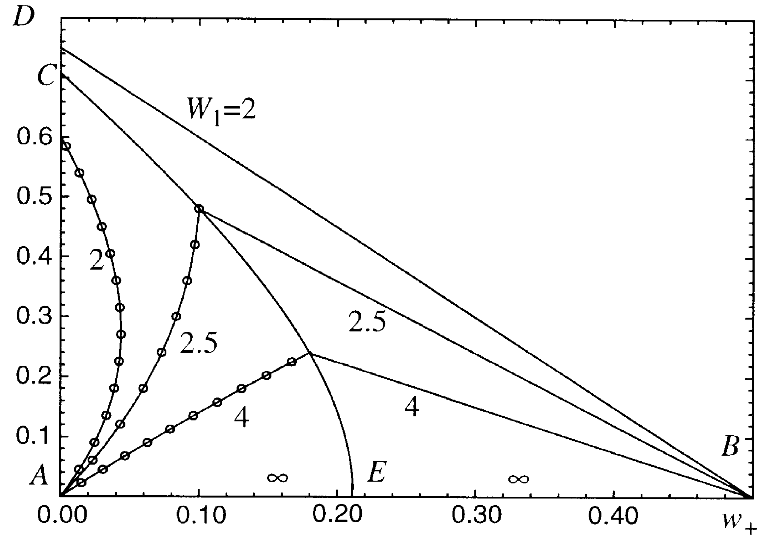

Fig. 3. Admissibility domains in the isothermal model at different values of w_1. The circles show numerical solutions of eqn (3.1) corresponding to kinks; it overlaps with the analytical solution of eqns (3.2) and (3.3) given by a solid line. Curve CE is the sonic line. In this figure $T_+ = 50$.

1982, 1987). As was shown by Rosakis (1995), the nonlinearity in the constitutive modelling of the viscoelastic properties of the media inside the transition front, can lead to more complicated isothermal kinetic behavior.

4.2. *Non-heat conducting medium* ($\mathbf{W}_2 = \infty$)

When the coefficient of heat conductivity tends to zero, the medium becomes non-heat conducting; physically this means that the process is adiabatic not only outside, but also inside the transition region. Notice that parameter $\boldsymbol{W}_2$ enters eqn (2.4) only in the combination $\boldsymbol{W}_2 D$. This suggests that in the limit of infinite $\boldsymbol{W}_2$ two cases have to be considered separately: $D \neq 0$ and $D = 0$.

Suppose first that $D \neq 0$. The energy equation reduces to an algebraic formula for the temperature

$$T = \left\{ -g(w) + g(w_+) + w_z^2 + \sigma(w_+, T_+)(w - w_+) + \tfrac{1}{2} D^2 (w - w_+)^2 \right\} + T_+,$$

and the main dynamical system is again two-dimensional

$$2w'' = -\boldsymbol{W}_1 D w_z + \boldsymbol{W}_3 w_z^2 - \boldsymbol{W}_3 \{g(w) - g(w_+)\} + \tfrac{1}{2} \boldsymbol{W}_3 D^2 (w - w_+)^2 + \boldsymbol{W}_3 \sigma(w_+, T_+)(w - w_+) + h(w) - h(w_+) - D^2 (w - w_+).$$

Here

$$g(w) \equiv w+\tfrac{1}{4}w^4-\tfrac{1}{2}w^3+\tfrac{1}{4}w^2, \quad h(w) \equiv 1+(w-1)(w)(w-\tfrac{1}{2}).$$

The structure of the admissibility set in this case is very similar to the one in the isothermal case up to a shift associated with the transition from isothermal to isoentropic stress-strain relation (which is no longer cubic). Kinetic curve and the boundary of the domain of shock admissibility can no longer be obtained analytically and were calculated numerically by a standard shooting procedure.

The results are presented in Fig. 4. The point A (w_+, T_+), where the kinetic curve crosses the $D = 0$ axis, corresponds to the adiabatic analog of the Maxwell condition (3.4)

$$\begin{aligned} &\sigma(w_-, T_-) = \sigma(w_+, T_+), \\ &e(w_-, T_-)-e(w_+, T_+) = \sigma(w_+, T_+)(w_- - w_+), \\ &s(w_-, T_-) = s(w_+, T_+). \end{aligned} \tag{3.5}$$

The adiabatic sonic line CE is given by the equation

$$D = a(w_+, T_+)$$

and is the analog of the isothermal sonic line discussed in the previous subsection. Again at the intersection of the kinetic curve AO with the sonic (Jouget) line CE, the shock admissibility boundary emerges (line OB). The area above COB represents the domain of admissible shocks, while the 'wedge region' EOB corresponds to the domain of non-admissible Lax shocks.

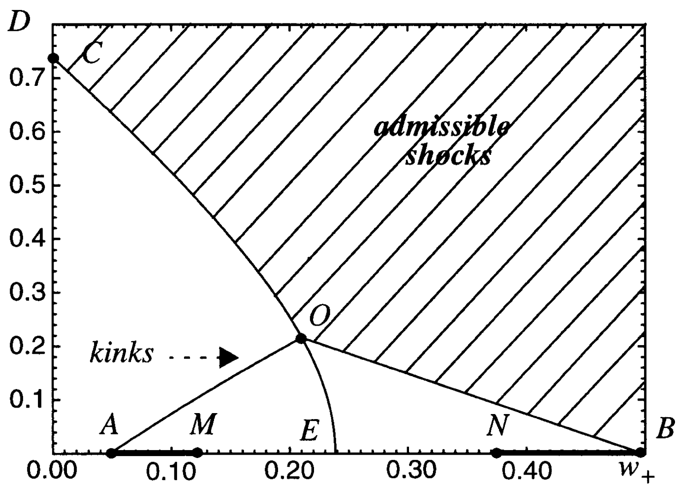

Fig. 4. A generic admissibility domain for the case of non-heat-conducting medium. The segment CE is the adiabatic sonic line, COB is the domain of admissible shocks, OAM is the kinetic curve for kinks; the segment AM corresponds to stationary kinks (contact discontinuities). In this figure $W_1 = 4$, $W_3 = 0.03$ and $T_+ = 50$.

Now, consider the limit $D \to 0$ as $\boldsymbol{W}_2 \to \infty$. Introduce a new parameter $\xi = D\boldsymbol{W}_2$ and suppose that it is finite in the limit. Equation (2.4) can be rewritten in the form

$$w'' = \tfrac{1}{2}\{\sigma(w, T) - \sigma(w_+, T_+)\},$$
$$T' = -\xi\{e(w, T) - e(w_+, T_+) - w'^2 - \sigma(w_+, T_+)(w - w_+)\}. \quad (3.6)$$

The boundary value problem for the system (3.6) was studied numerically and the spectrum of admissible ξ is shown in Fig. 5. Heteroclinic trajectories corresponding to kinks exist in a finite range of strains w_+ represented in Fig. 4 by the segment AM; these kinks are stationary and represent a sub-branch of contact discontinuities. Contrary to the isothermal case, where stationary kinks were necessarily Maxwellian—see conditions (3.4), now there exists a one-parametric family of stationary solutions. These kinks cannot move because of the system's inability to remove the latent heat of the transformation: an infinitesimal heat release leads to an increase of local temperature and accordingly the transformation stress which blocks the transformation (thermal trapping).

From Fig. 5 one can see that the stationary solution is not unique around point M: the emerging loops correspond to kinks with non-monotone internal structure. The nature of the point M, whose location depends on $\boldsymbol{W}_3$ only, and the origin of the multiplicity of solutions around this point will become more clear from the next section where the general case is considered. The exact location of point M is calculated analytically in the next sub-section.

The variation of the nondimensional parameter $\boldsymbol{W}_1$ causes predictable distortions of the admissibility domain that can essentially be read from Fig. 3. The location of the points A, M, E and C remain unchanged.

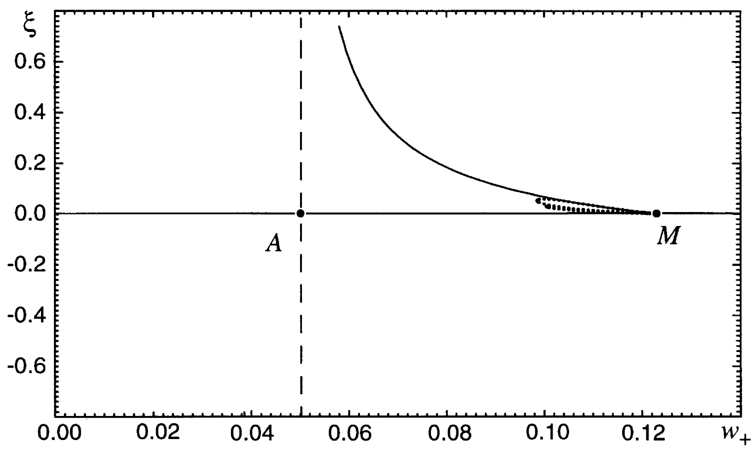

Fig. 5. The dependence of $\xi = D\boldsymbol{W}_2$ versus w_+ for stationary kinks in non-heat-conducting medium. Points A and M are the same as in Fig. 4. Loops around point M correspond to stationary kinks with nonmonotone internal structure. In this figure $\boldsymbol{W}_1 = 4$, $\boldsymbol{W}_3 = 0.03$ and $T_+ = 50$.

4.3. *Infinitely heat-conductive medium* ($\mathbf{W}_2 = 0$)

Now, consider another important special case when the coefficient of heat conductivity is large. This asymptotics, studied by Slemrod (1984) and Truskinovsky (1985) in the context of van der Waals fluids, and by Turteltaub (1997) for the trilinear material, becomes relevant when the thickness of the thermal boundary layer is much larger than the internal length scale of the medium.

As was first shown by Slemrod (1984), in the limit $\boldsymbol{W}_2 \to 0$, the actual phase transformation takes place almost isothermally in a region scaled with $\sqrt{\varepsilon}$, while the process of the latent heat redistribution takes place in an adjacent thermal boundary layer of much larger thickness, κ/c. To verify this picture, consider a two-scale asymptotic expansion of the system (2.4). At the scale $z \sim 0(1)$ we obtain

$$w'' = \tfrac{1}{2}[\sigma(w, T) - \sigma(w_+, T_+) - \boldsymbol{W}_1 D w_z - D^2(w - w_+)], \quad T' = 0. \tag{3.7}$$

These equations, which govern the behavior of the system inside the transition layer, are identical to eqn (3.1) with the solution available in closed form. To obtain the outer expansion, introduce a stretched coordinate $\tilde{z} = \boldsymbol{W}_2 z$. Now, in the limit $\boldsymbol{W}_2 \to 0$, the system (2.4) takes the form

$$\begin{aligned} 0 &= \sigma(w, T) - \sigma(w_+, T_+) - D^2(w - w_+), \\ T_{\tilde{z}} &= -D\{e(w, T) - e(w_+, T_+) - \tfrac{1}{2}\{\sigma(w_+, T_+) + \sigma(w, T)\}(w - w_+)\}. \end{aligned} \tag{3.8}$$

This system is one-dimensional and is easy to analyze. For example, eqn (3.8_1) means that the phase trajectory follows the Rayleigh line, while eqn (3.8_2) states that the temperature is a decreasing or increasing function depending on whether one is above or below the Hugoniot curve. The internal structure of the kink moving to the right ($D \geqslant 0$) is illustrated in Fig. 6. The solution consists of an isothermal transition CB and a thermal boundary layer BA in front of it.

The problem of calculating the kinetic relation is now algebraic. In fact, suppose that the state at $z = +\infty$, is given—point A with coordinates (w_+, T_+). Since the points A and C in Fig. 6 represent configurations in front and behind the adiabatic discontinuity, their coordinates must satisfy the Rankine-Hugoniot conditions

$$\begin{aligned} 0 &= e(w_-, T_-) - e(w_+, T_+) - \tfrac{1}{2}\{\sigma[w_+, T_+) + \sigma(w_-, T_-)\}(w_-, T_-), \\ 0 &= \sigma(w_-, T_-) - \sigma(w_+, T_+) - D^2(w_- - w_+). \end{aligned} \tag{3.9}$$

These two equations contain three unknowns. To obtain a missing condition, one simply needs to apply eqn (3.3) which can be rewritten as

$$D = \frac{3}{\boldsymbol{W}_1}\left\{ w_- + \frac{1}{-36 + 4\boldsymbol{W}_1^2}(-36 + 36w_- + 3\boldsymbol{W}_1^2 - 2w_-\boldsymbol{W}_1^2 \right.$$
$$\left. \pm \boldsymbol{W}_1\sqrt{-144w_- + 144w_-^2 + \boldsymbol{W}_1^2 + 12w_-\boldsymbol{W}_1^2 - 12w_-^2\boldsymbol{W}_1^2}] - 1 \right\}.$$

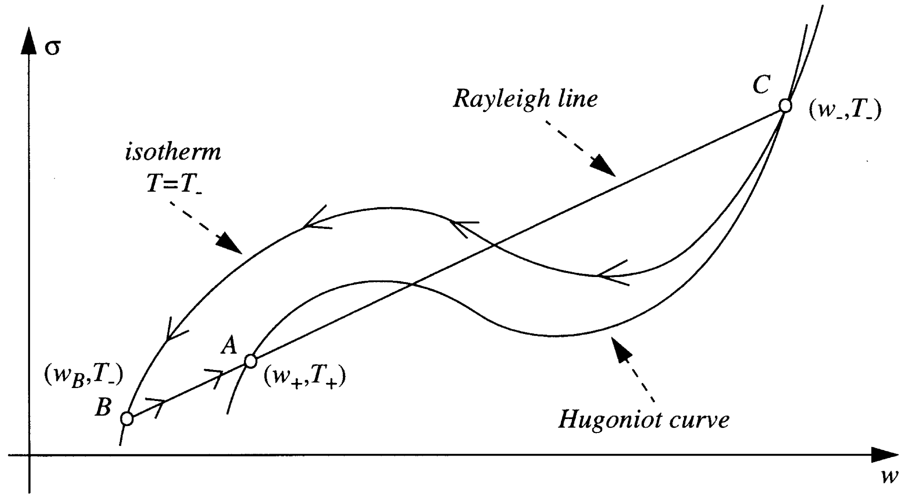

Fig. 6. A generic structure of a kink in the infinitely heat conducting medium. The isothermal segment of the solution corresponds to the trajectory from point C to point B. All of the temperature variation occurs in the second segment, which starts from point B, continues along the Rayleigh line, and ends at point A. Point C lies on the Hugoniot adiabat originating at point A.

This relation together with eqn (3.9) allows one to find the three unknowns w_-, T_- and D. The calculated admissibility domains at various W_1 and W_3 are presented in Fig. 7.

One can see that kinetic curves corresponding to the same W_3 and different W_1 intersect the horizontal axis of the $w_+ - D$ plane at a single point; it is not difficult to

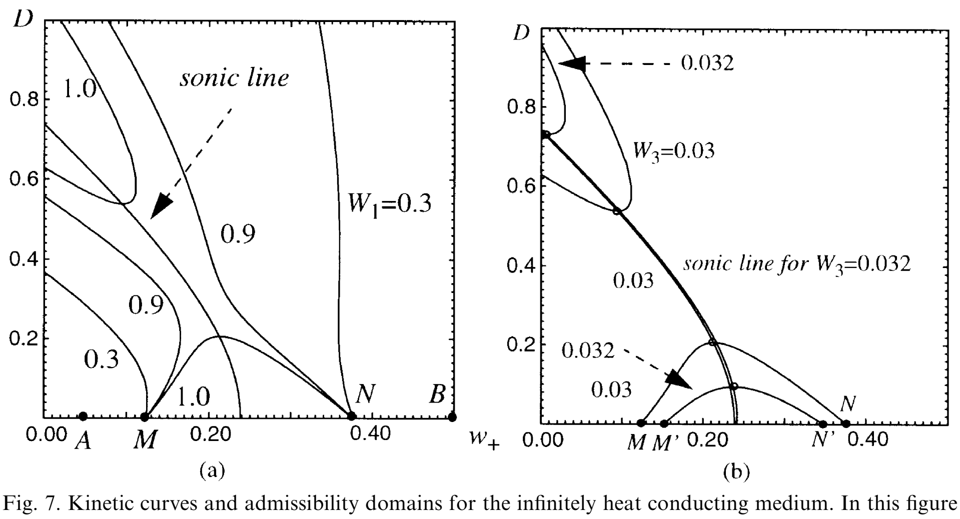

Fig. 7. Kinetic curves and admissibility domains for the infinitely heat conducting medium. In this figure $W_3 = 0.03$(a) and $W_1 = 1$(b); $T_+ = 50$.

show that this point coincides with the point M mentioned in the previous subsection. To calculate the coordinates of point M we notice that at $D = 0$ the state behind the phase boundary must be at the Maxwell stress corresponding to T_-. Therefore, the following equation must be satisfied

$$\sigma(w_-, T_-) = \sigma(w_+, T_+), \quad e(w_-, T_-) - e(w_+, T_+) = \sigma(w_+, T_+)(w_- - w_+). \tag{3.11}$$

Here w_- denotes the displacement gradient in the high strain phase corresponding to Maxwell stress at temperature T_-; under our constitutive assumptions, $w_- = 1$. The system of two eqns (3.11) with the two unknowns w_+ and T_- allows one to locate the point M for any given $\boldsymbol{W}_3$ and T_+.

The internal structure of the kink at $D = 0$ (point M in fig. 7) can be read from Fig. 6. All three points, A, B and C, are now at zero stress; moreover, points B and C describe two phases in thermodynamic equilibrium. This suggests that arbitrary oscillations between the equilibrium (Maxwell) points B and C can be added to the solution without modifying any of the equations. As a result, the configuration with a single interface is not unique and phases may mix inside the transition front. The implications of this observation are further elaborated in the next section where the degeneracy of the present asymptotics is removed.

The last observation concerns the passibility of splitting, as viscosity gets larger, of the kinetic curve into two disjoint segments (slow and fast kinks), which is accompanied by a change in the topology of the domain of admissible shocks (see Fig. 7).

5. General case

In this section we present numerical results for the general case of heat conducting medium with nonzero latent heat. We will vary independently the nondimensional parameters $\boldsymbol{W}_1$, $\boldsymbol{W}_2$ and $\boldsymbol{W}_3$.

We begin with the parameter $\boldsymbol{W}_2$, which measures the effectiveness of the heat removal. As we change $\boldsymbol{W}_2$ from 0 to ∞, the structure of the admissibility domain containing: (i) 1D segment corresponding to kinks (kinetic curve) and (ii) 2D domain of admissible shocks, varies continuously from the one discussed earlier for the infinitely heat conductive medium ($\boldsymbol{W}_2 = 0$), to the one for the non-heat conducting medium ($\boldsymbol{W}_2 = \infty$). A specific example is presented in Fig. 8 where parameters $\boldsymbol{W}_1$ and $\boldsymbol{W}_3$ are held fixed.

One can make the following observations. For $\boldsymbol{W}_3$ given, all kinetic curves originate from the same point M whose exact location has been calculated in the previous section. The peculiar status of the limiting case $\boldsymbol{W}_2 = \infty$ becomes more clear: the singular branch of stationary kinks obtained for non-heat-conducting medium ($\boldsymbol{W}_2 = \infty$) becomes a regular part of the $1D$ set of admissible kinks for $0 < \boldsymbol{W}_2 < \infty$ and the corresponding contact discontinuities turn into slowly moving kinks. As parameter $\boldsymbol{W}_2$ gets smaller, the kinetic curve approaches the limit of an infinitely heat

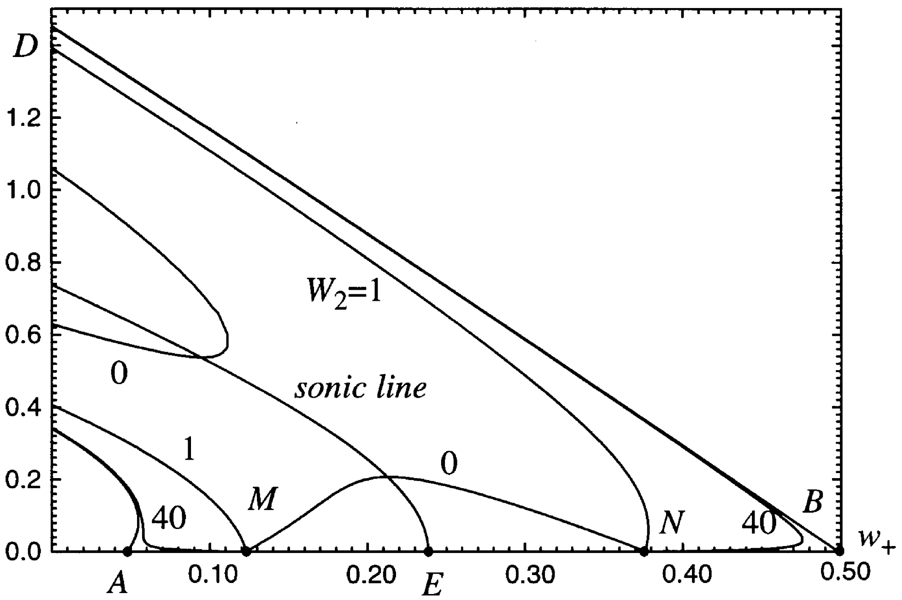

Fig. 8. The W_2 dependence of the admissibility region for the general case of heat conducting medium. In this figure $W_1 = 1$, $W_3 = 0.03$ and $T_+ = 50$.

conducting medium which is represented in this case by two disjoint segments. The boundary of the shock admissibility region splits accordingly (see Fig. 8).

We observe that when the coefficient of heat conductivity is small, the low velocity part of the kinetic curve is non-monotone. A close look at the structure of the kinetic curves around point M reveals even more complicated behavior shown in Fig. 9. Recall that our analyses in the previous section have provided some indications of the existence of multiple non-monotone solutions emerging around this point: the numerical calculations for the general case confirm that in the vicinity of point M, there exists a finite family of nontrivial kinks. The loops on the kinetic curve accumulate as one gets closer to point M (with only few of the loops shown in Fig. 9).

The behavior of the corresponding trajectories in the phase space is shown in Fig. 10: nontrivial solutions are characterized by oscillations of strain in the transitional region and describe mixing of the two phases within the phase boundary structure. The number of phase switches increases as we go from point P to point R (see Figs 9 and 10). The temperature field inside the phase boundary is also nonmonotone with the spikes marking internal transitions between the phases. Physically, the phenomenon of internal mixing originates from the interplay between the tendency towards formation of the second phase and the blocking influence of the heat release. As heat conductivity increases, the loops get smaller: in the limiting case $W_2 = 0$ the loops are confined to a single point M. In the other limiting case, $W_2 = \infty$, the loops are represented by a family of contact discontinuities.

With parameter W_2 decreasing, the kinetic curve bends in the direction of the

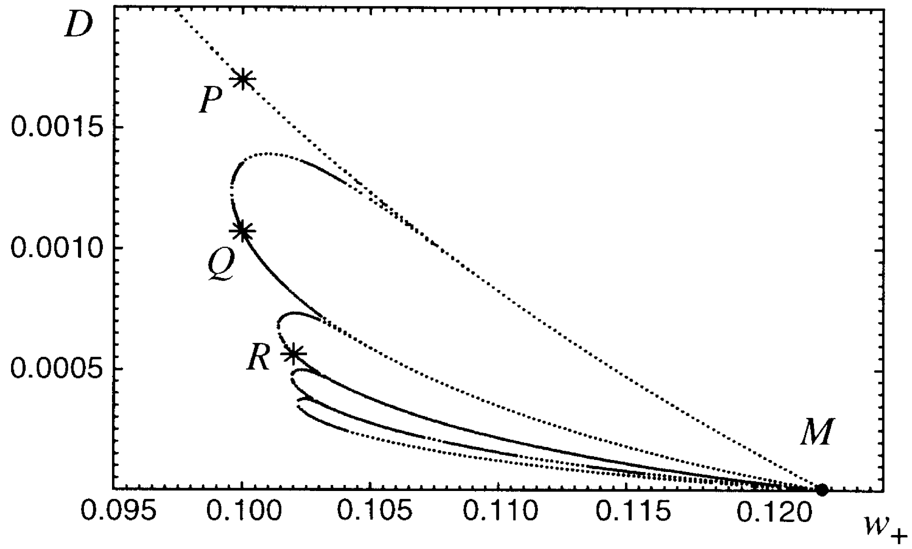

Fig. 9. A fragment of Fig. 8 showing the multiplicity of kinks and the corresponding loops on the kinetic curve around point M. In this figure $W_1 = 1$, $W_2 = 40$, $W_3 = 0.03$ and $T_+ = 50$. The detailed structure of the solutions at points P, Q and R is shown in Fig. 10.

sonic line (see Fig. 9) and eventually touches it. Simultaneously the line separating admissible and non-admissible kinks also touches the sonic line at the same point. The topology of the admissible region changes, which leads to the formation of two disjoint branches of kinks (slow and fast) and two disjoint regions of non-admissible kinks.

The role of parameter W_3 is illustrated in Fig. 11. The kink-type solutions exist for a finite range of W_3 only. When W_3 tends to zero, the kinetic curve approaches the analytic solution for the isothermal problem. As parameter W_3 increases, which happens for instance, when the specific heat decreases, the Hugoniot adiabat eventually becomes convex and kinks disappear. An interesting topological restructuring of the admissibility domain takes place before that, when at some value of $W_3 = W_3^*$ points M and E overlap. For $W_3 > W_3^*$ the kinetic curve does not cross the $D = 0$ axis so that slow kinks cease to exist (see Fig. 11). Beginning from this value of W_3, the kinetic curve begins and ends at the sonic line (see Fig. 12). This behavior differs in a qualitative way from the conventional picture of the isothermal kinetics when slow kinks obey the so-called 'normal growth' law (e.g. Truskinovsky, 1994a).

6. Mobility curves

As we mentioned in Section 1, an additional jump condition selecting admissible kinks is often formulated as a particular functional expression for the rate of entropy production at a moving interface (e.g. Abeyaratne and Knowles, 1991; Gurtin, 1993;

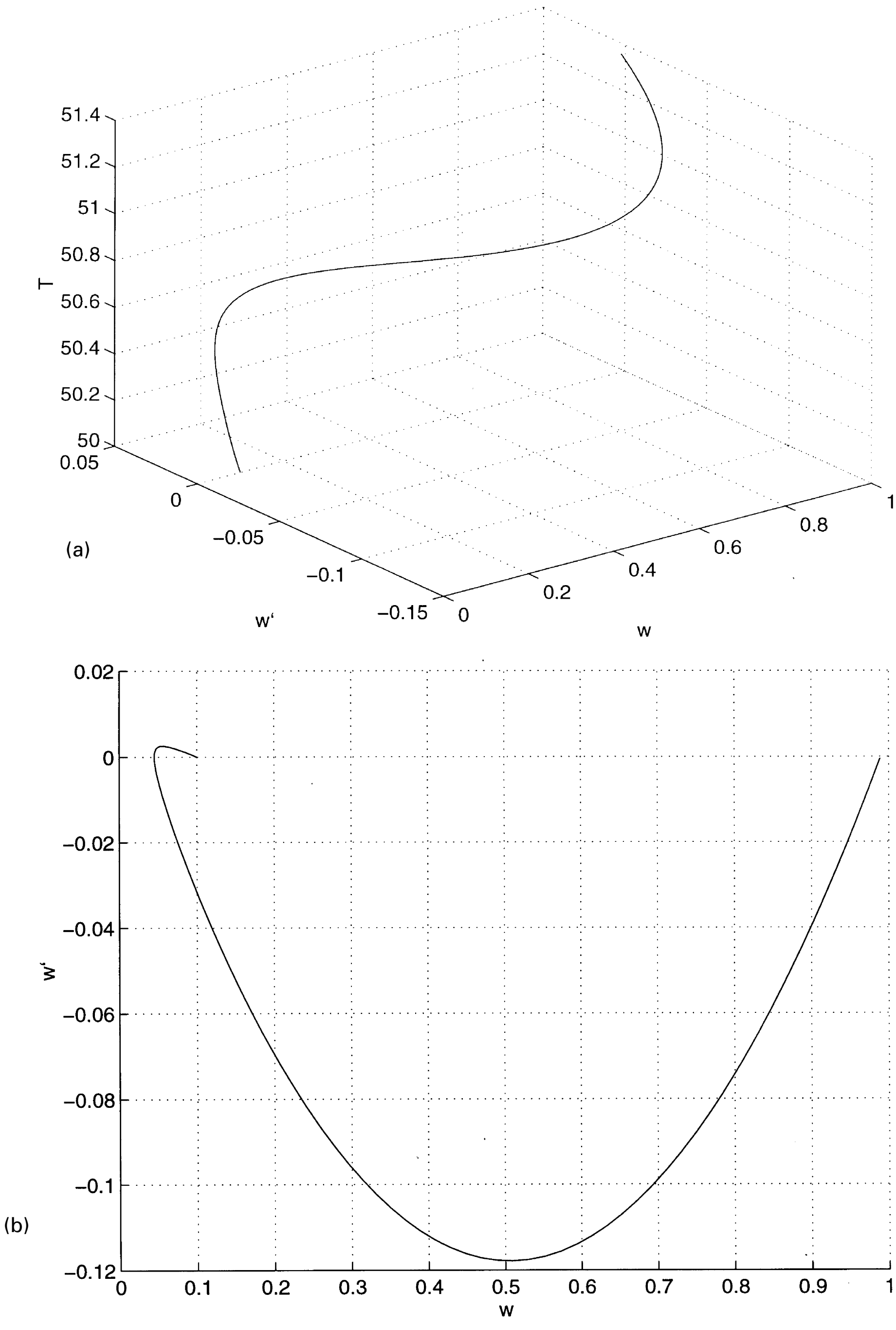

Fig. 10. Fine structure of the adiabatic kinks corresponding to the points P (a,b,c), Q (d,e,f) and R (g,h,i) from Fig. 9. The corresponding heteroclinic trajectory is shown in the 3D phase space T–w′–w. Also shown are the two projections into w′–w space and into T–w space.

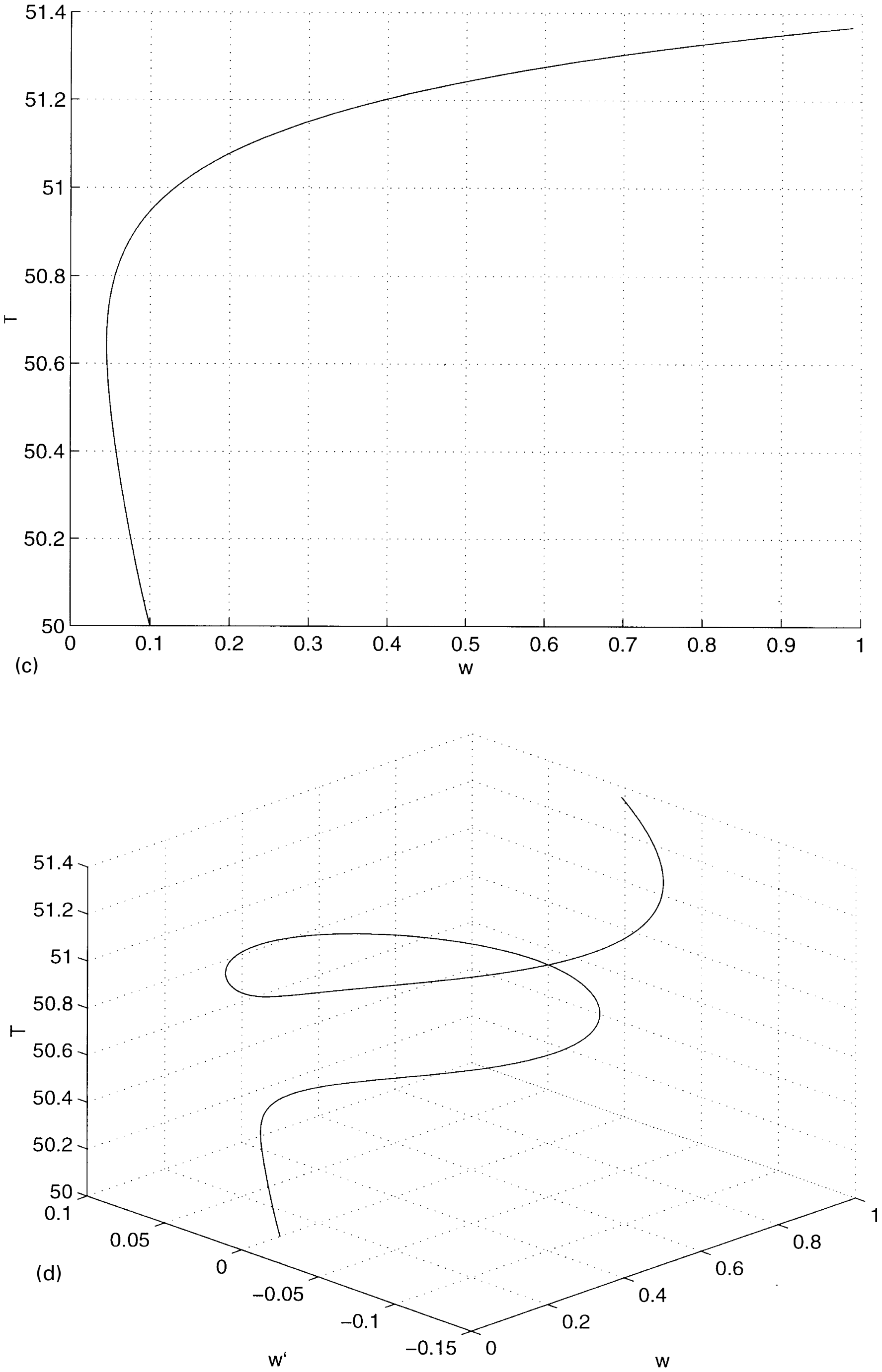

Fig. 10. *Continued.*

(e)

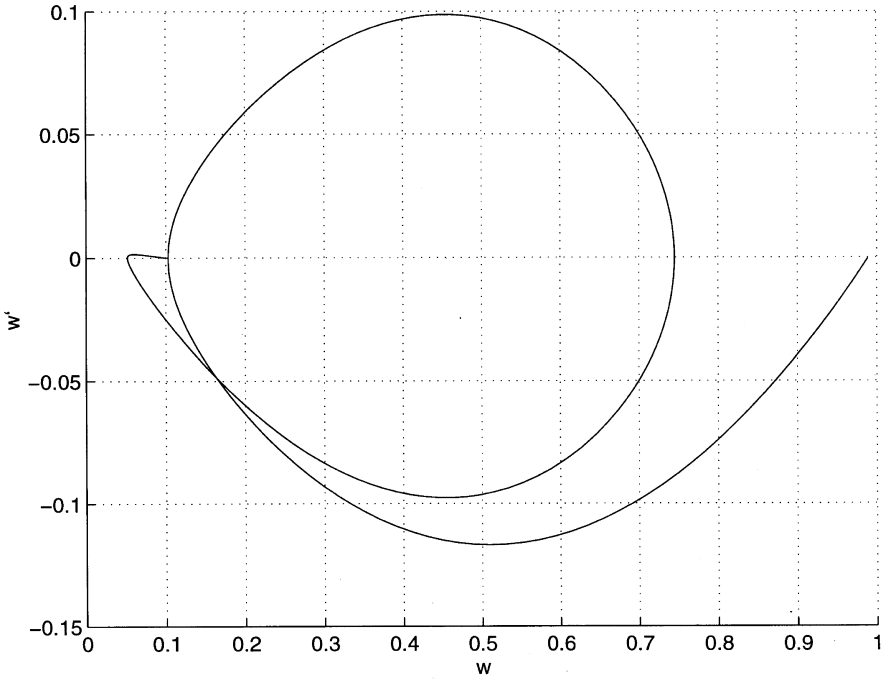

(f)

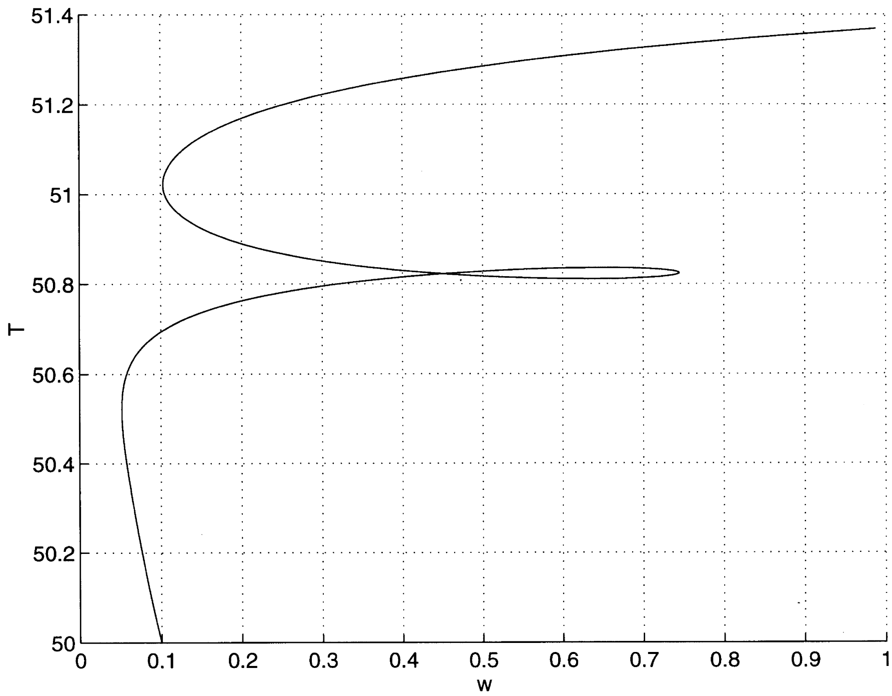

Fig. 10. *Continued.*

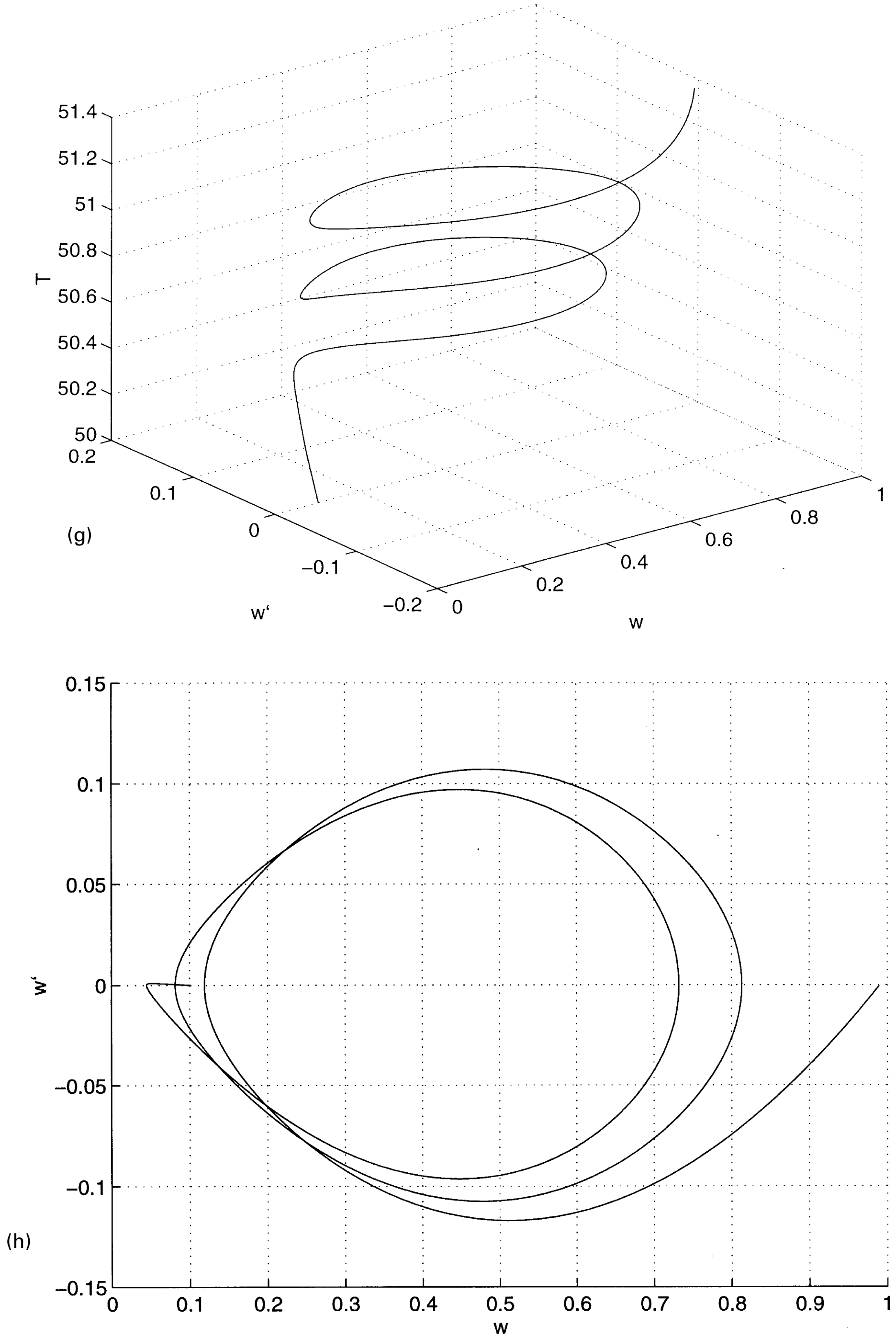

Fig. 10. *Continued.*

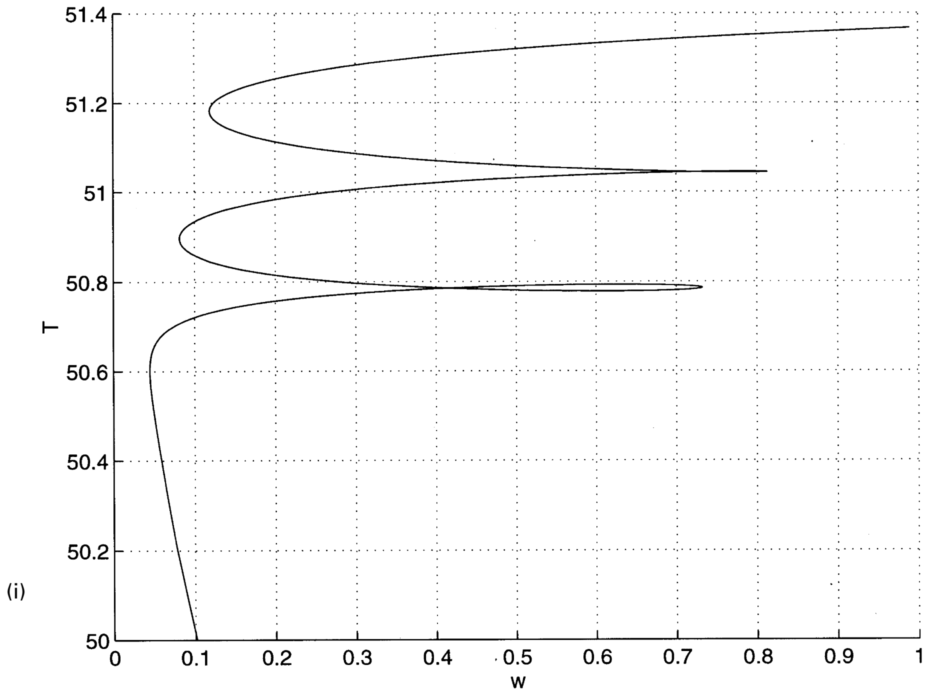

Fig. 10. *Continued.*

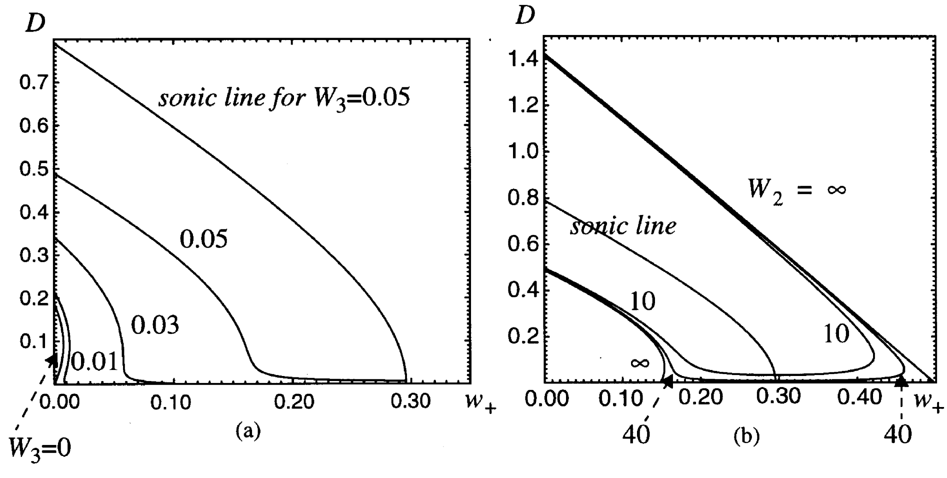

Fig. 11. Kinetic curves and shock admissibility domains for the general heat conducting medium: the role of parameter W_3. In figure (a) $W_1 = 1$, $W_2 = 40$ and $T_+ = 50$. In figure (b) $W_1 = 1$, $W_3 = 0.05$ and $T_+ = 50$.

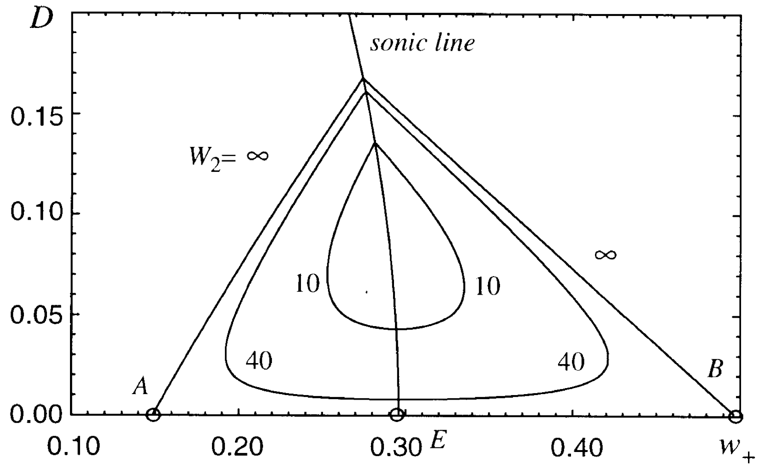

Fig. 12. Kinetic curves and shock admissibility domains for the general heat conducting medium: the role of parameter W_2. In this figure $W_1 = 4$, $W_3 = 0.05$ and $T_+ = 50$.

Truskinovsky, 1987). In this section we will adopt this point of view and will reformulate the kinetic relations, calculated at the fixed W_1, W_2 and W_3, in terms of the relation between $G \equiv -[s]$, the 'driving force', and D, the conjugate 'flux'. Kinetic curves represented in this way will be called mobility curves. A certain difficulty with the presentation of the kinetic curves in the D–G space is related to the fact that the mapping $(D, w_+) \rightarrow (D, G)$ is not one-to-one with a fold at sonic line. We also remark that our kinetic relations can only be represented in terms of a relation between two variables when one of the parameters of the flow is fixed. In the discussion below it will be the temperature ahead of the kink, T_+.

The W_2 dependence of the mobility curves for the general case of heat conducting medium is shown in Fig. 13. We observe that the mobility curves, corresponding to different values of W_2 converge as $D \rightarrow 0$ to point M (same as point M in Fig. 8). The driving force G at this point is different from zero which means that the rate of dissipation $\Re = DG$ (dissipative potential) as a function of D is not quadratic but rather linear at zero velocities. At large W_2 (small heat conductivity), the mobility curves become non-monotone; closer examination around point M reveals the already familiar loop structures. Since the nonmonotonicity in the D–G plane reflects the nonconvexity of the dissipative function, the kinks corresponding to the descending branches of the mobility curve are most probably unstable. As W_2 decreases the mobility curves shift upward because the rise in thermal conductivity increases thermal dissipation and higher driving traction is needed to maintain the same phase boundary velocity. The same basic trend is observed when parameter W_1 is varied.

The structure of the admissibility domain strongly depends on W_3. As W_3 increases, first, slow kinks disappear and the starting point for the mobility curves moves on a sonic line. Further increase in W_3 results in a complete disappearance of both kinks and non admissible shocks (see Fig. 14).

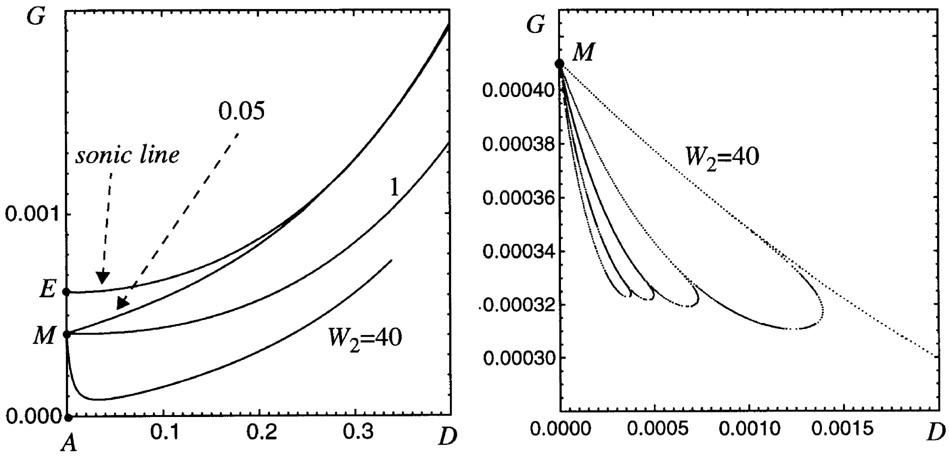

Fig. 13. Mobility curves at different W_2 for the general case of heat conducting medium. The picture on the right is a close up view of the loop structures around point M for one of these curves ($W_2 = 40$). In this figure $W_1 = 1$, $W_3 = 0.03$ and $T_+ = 50$.

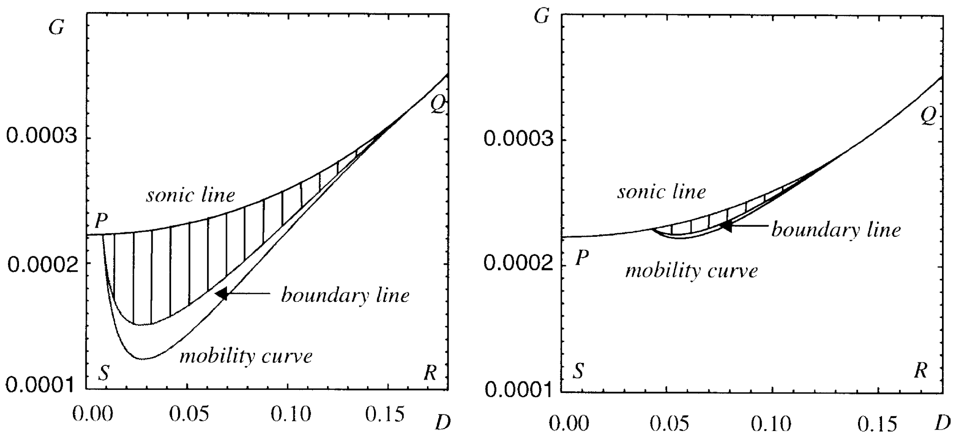

Fig. 14. The structure of the admissibility domain in the D–G space for a general case of heat conducting medium. The region below the sonic line, except for the shaded area, corresponds to the domain of admissible shocks. In this figure: (a) $W_1 = 4$, $W_2 = 40$, $W_3 = 0.05$ and $T_+ = 50$; (b) $W_1 = 4$, $W_2 = 10$, $W_3 = 0.05$ and $T_+ = 50$.

The question that remains concerns the role of the temperature ahead of the discontinuity; this parameter was held fixed in all numerical experiments so far. Our Fig. 15 shows how the kinetic curves in the w_+–D space and the corresponding mobility curves in the D–G space vary as we change the temperatures of the state in front. The figure shows that the influence of T_+ is similar to the effect of W_3 and cannot be neglected. The fact that the mobility curves show strong dependence on the temperature in front suggests that the information about kinetics cannot be

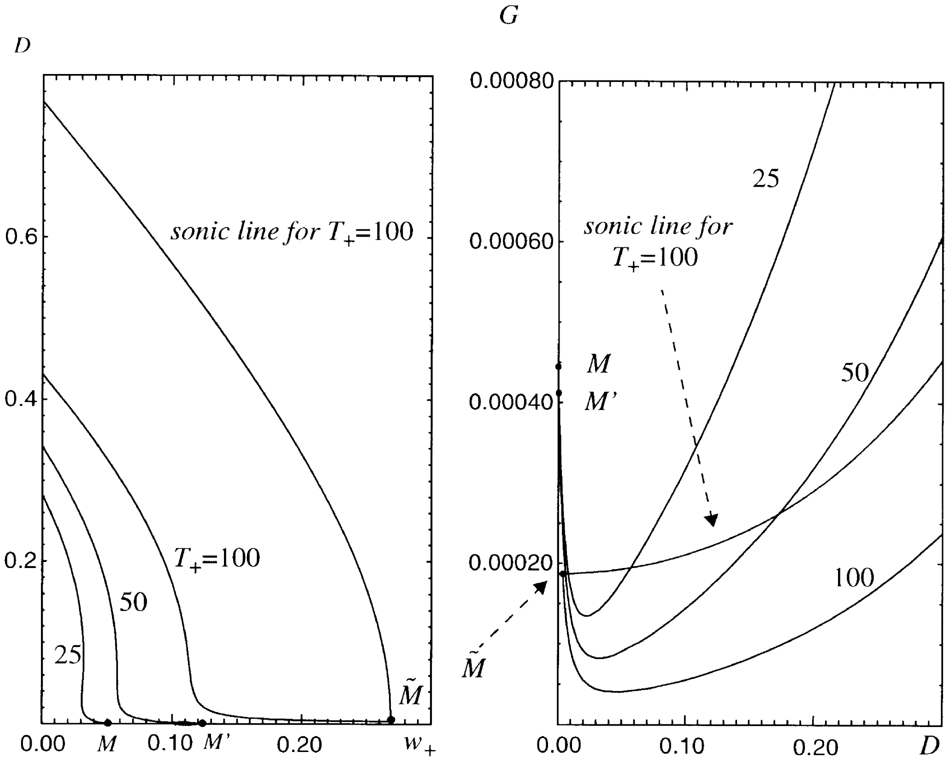

Fig. 15. Kinetic curves and the corresponding mobility curves for the general case of heat conducting medium: the role of T_+. Point $\tilde{M}$ marks the intersection of the kinetic curve with the sonic line. In this figure $\boldsymbol{W}_1 = 1$, $\boldsymbol{W}_2 = 40$, $\boldsymbol{W}_3 = 0.03$.

compressed into a relation of the type in eqn (1.6). Our attempts to find a relation of the form of eqn (1.7), compatible with the calculated mobility curves, were also unsuccessful.

7. Discussion

In this paper we studied traveling wave solutions in the non-isothermal viscosity–capillarity model, which includes the Stefan problem, as well as purely mechanical inertial problem, as special cases. By analyzing the structure of the transition front, we obtained detailed information about the kinetics of adiabatic phase boundaries. In particular, we have demonstrated that the admissible region in the space of parameters has a complicated topology and consists of pieces with different spatial dimensions. We have shown that at low velocities the kinetic relations are non-monotone and non-single-valued. This result is incompatible with the popular 'normal growth' type assumptions which are often used to phenomenologically 'correct' Stefan's formulation.

Our interest in the temperature effects was independently motivated by numerical experiments with discrete lattices made of bi-stable elements (Ngan and Truskinovsky, 1998). We observed that solutions of discrete models are highly oscillatory so that the classical waves may be interpreted as weak limits at most. Analyses of the static problem have shown that the typical energy landscape of a bi-stable chain is 'bumpy' and possesses multiple isolated local minima (see, for instance, Rogers and Truskinovsky, 1997). As a consequence, in order to move a phase boundary in a discrete lattice one has to overcome a succession of potential barriers which are formally absent in the classical elastodynamical setting. Our numerical experiments demonstrated massive energy transfer from long to short scales as the 'switching' wave propagated through the sample, the phenomenon studied earlier by Slepyan and Troyankina (1984) in the context of dynamic fracture. The presence of elastic radiation at micro scales suggests that the interaction between continuum and subcontinuum levels can not be described in terms of purely mechanical variables, and that it is essential to consider what one can loosely call 'thermal' effects (see von Neumann, 1944, for some early insights). Moreover, an adequate continuum model of phase transition must also describe inertia, associated with the activation of an 'invisible' motion at the microlevel. Simulation of these phenomena is impossible without new variables describing the level of fluctuations, the rate of energy flux into the microlevel and back, and the rate of irreversible dissipation by radiation.

Comprehensive dynamical homogenization of the bi-stable lattices represents a highly nontrivial mathematical problem. Our introduction of a temperature field can be viewed as an attempt to track the energy of the high frequency oscillations phenomenologically. Although classical heat conductivity is hardly a universal description of the propagation of high-frequency vibrations in nonlinear lattices, our kinetic relations turn out to be surprisingly similar to the ones obtained by Slepyan and Trojankina (1984) and Slepyan (1996) from the analysis of the waves that carry the energy away from the failure front (see also Marder and Gross, 1995, for a discussion of a related model). These authors calculated the analogs of kinetic curves for the kinks in a bi-linear discrete system, and demonstrated that they possess the same qualitative features as our mobility curves: nonmonotonicity, multiplicity of branches and trapping. The quantitative comparison depends on the value of the latent heat of the transformation. While in the theory of phase transformations, the meaning of the latent heat is clear, it is not at all obvious how to calculate this parameter for the purely mechanical chain.

What may be most interesting is the extension of these ideas to fracture. The analogy suggests the following conclusions:

(i) The macroscopic dynamic fracture cannot be described in purely mechanical terms.
(ii) In addition to the energy release rate, there is a nonzero latent heat of fracture.
(iii) 'Heat' removal may be a rate limiting process and may even block the propagation of a crack.

The validity of these conjectures can be tested through the careful study of discrete models as well as through direct measurements of the localized heat effects.

Acknowledgements

This work was supported by the NSF grant DMS-9501433.

References

Abeyaratne, R., Knowles, J.K., 1991a. Kinetic relations and the propagation of phase boundaries in solids. Arch. Rat. Mech. Anal. 114, 119–154.

Abeyaratne, R., Knowles, J.K. 1991b. Implications of viscosity and strain-gradient effects for the kinetics of propagating phase boundaries in solids. SIAM J. Appl. Math. 51, 1205–1221.

Abeyaratne, R., Knowles, J.K., 1994a. Dynamics of propagating phase boundaries: thermoelastic solids with heat conduction. Arch. Rat. Mech. anal. 126, 203–230.

Abeyaratne, R., Knowles, J.K., 1994b. Dynamics of propagating phase boundaries: adiabatic theory for thermoelastic solids. Physica D 79, 269–288.

Bruno, O.P., Leo, P.H., Reitich, F., 1995. Free boundary conditions at austenite–martensite boundary. Phys. Rev. Lett. 74 (5), 746.

Ericksen, J.L., 1975. Equilibriumn of bars. J. Elasticity 5, 191–202.

Freund, L.B., 1990. Dynamic fracture mechanics. Cambridge University Press, Cambridge.

Garcke, H., 1995. Traveling wave solutions as dynamic phase transitions in shape memory alloys. J. Diff. Eq. 121, 203–231.

Grinfield, M., 1989. Nonisothermal dynamic phase transitions. Quart. Appl. Math. XLVII, 1, 71–84.

Gurtin, M.E., 1993. The dynamics of solid-solid phase transitions 1. Coherent interfaces. Arch. Rat. Mech. Anal. 123, 305–335.

Kulikovsky, A.G., 1976. On the discontinuous solutions in mechanics of continuous media. In: Koiter, W.T. (Ed.), Theoretical and Applied Mechanics, North Holland.

Lax, P.D., 1971. Shock waves and entropy. In: Zarantonello, E.A. (Ed.), Contributions to Nonlinear Functional Analysis. Academic Press, NY.

Leo, P.H., Shield, T.W., Bruno, O.P., 1993. Transient heat transfer effects on the pseudoelastic behavior of shape-memory wires. Acta Metallurgica 41 (8), 2477–2485.

Malomed, B.A., Rumanov, E.N., 1985. Natural velocity of the boundary between phases. Sov. Phys. Dokl. 30 (10), 872–874.

Marder, M., Gross, S., 1995. Origin of crack tip instabilities. J. Mech. Phys. Solids 43, 1–48.

Neumann, von, J., 1944. Proposal and analysis of a new numerical method in the treatment of hydrodynamical shock problem. Vol. VI, Collected works. Pergamon, London.

Ngan, S.C., Truskinovsky, L., 1997. Dynamic nucleation in thermoelastic solids. To be submitted.

Patashinskii, A.Z., Chertkov, M.V., 1990. Motion of the front of a phase transition under strong supercooling conditions. Sov. Phys. Solid State 36, 295–299.

Pego, R., 1987. Phase transitions in a one dimensional nonlinear viscoelasticity: admissibility and stability. Arch. Rat. Mech. Anal. 97, 353–394.

Rogers, R., Truskinovsky, L., 1997. Discretization and hysteresis. Physica B 233, 370–375.

Rosakis, P., 1995. An equal area rule for dissipative kinetics of propagating strain discontinuities. SIAM J. Appl. Math. 55 (1), 100–123.

Rosakis, P., Knowles, J.K., 1997. Unstable kinetic relations and the dynamics of solid-solid phase transitions. J. Mech. Phys. Solids 45 (11/12), 1055–2081.

Shaw, J.A., Kiriakides, S., 1995. Thermomechanical aspects of NiTi. J. Mech. Phys. Solids 43, 1243–1281.

Shield, T.W., Leo, P.H., Grebner, W.C.C., 1997. Quasi-static extension of shape memory wires under constant load. Acta Mater. 45 (1), 67–74.

Shearer, M., 1982. The Reimann problem for a class of conservation laws of mixed type. J. Diff. Eq. 46, 426–443.

Shearer, M., Yang, Y., 1995. The Reimann problem for a system of conservation laws of mixed type with cubic nonlinearity. Proc. Roy. Soc. Edinburgh A. 125A, 675–699.

Slemrod, M., 1983. Admissibility criteria for propagating phase boundaries in a Van der Waals fluid. Arch. Rat. Mech. Anal. 81, 301–315.

Slemrod, M., 1984. Dynamic phase transitions in a Van der Waals fluid. J. Diff. Eqs. 52, 1–23.

Slepyan, L.I., 1996. Crack dynamics. In: Cherepanov, G. (Ed.), Fracture: A topical encyclopedia of current knowledge. Krieger, Melbourne, 631–670.

Slepyan, L.I., Trojankina, L.V., 1984. Fracture wave in a chain structure. J. Appl. Mech. Techn. Phys. 25 (6), 921–927.

Truskinovsky, L., 1982. Equilibrium phase boundaries. Sov. Phys. Doklady 27, 551–553.

Truskinovsky, L., 1985. Structure of an isothermal phase jump. Sov. Phys. Doklady 30, 945–948.

Truskinovsky, L., 1987. Dynamics of nonequilibrium phase boundaries in a heat conducting nonlinear elastic medium. J. Appl. Math. and Mech. (PMM) 51, 777–784.

Truskinovsky, L., 1993. Kinks versus shocks. In: Fosdick, R., Dunn, E., Slemrod, M. (Eds), Shock Induced Transitions and Phase Structures in General Media. IMA 52, Springer–Verlag, New York.

Truskinovsky, L., 1994a. About the normal growth approximation in the dynamical theory of phase transitions. Continuum Mechanics and Thermodynamics 6, 185–208.

Truskinovsky, L., 1994b. Transition to detonation in the dynamic phase changes. Arch. Rat. Mech. Anal. 125, 375–397.

Truskinovsky, L., 1996. Fracture as a phase transition. In: Batra, R.C., Beatty, M.F. (Eds), Contemporary research in the mechanics and mathematics of materials. A collection of papers dedicated to the 70th birthday of J. Ericksen. CIMNE, Barcelona, pp. 322–332.

Truskinovsky, L., 1997. Nucleation and growth in classical elastodynamics. In: Duxbury, P.M., Pence, T. (Eds.), Dynamics of Crystal Surfaces and Interfaces. Fundamental Materials Science Series, Plenum, New York, pp. 185-197.

Turteltaub, S., 1997. Viscosity and strain gradient effects on the kinetics of propagating phase boundaries in solids. J. Elast. 46 (1), 53–90.

Umantsev, A., 1992. Thermodynamic stability of phases and transition kinetics under adiabatic conditions. J. Chem. Phys. 96, 605–617.

Zhong, X., Batra, R.C., 1996. Modeling of macroscopic response of phase transforming materials under quasi-static loading. J. Elast. 44, 145–160.